Short-range order in a steady state of irradiated Cu-Pd alloys: comparison with fluctuations at thermal equilibrium

1998 J. Phys.: Condens. Matter 10 3791

(http://iopscience.iop.org/0953-8984/10/17/011)

J. Phys.: Condens. Matter **10** (1998) 3791–3806. Printed in the UK PII: S0953-8984(98)90924-9

Short-range order in a steady state of irradiated Cu–Pd alloys: comparison with fluctuations at thermal equilibrium

I Tsatskis† and E K H Salje

Department of Earth Sciences, University of Cambridge, Downing Street, Cambridge CB2 3EQ, UK

Received 21 January 1998

Abstract. The equilibrium short-range order (SRO) in Cu–Pd alloys is studied theoretically. The evolution of the Fermi surface-related splitting of the (110) diffuse intensity peak with changing temperature is examined. The results are compared with experimental observations for electron-irradiated samples in a steady state, for which the temperature dependence of the splitting was previously found in the composition range from 20 to 28 at.% Pd. The equilibrium state is studied by analysing available experimental and theoretical results and using a recently proposed alpha-expansion theory of SRO which is able to describe the temperature-dependent splitting. It is found that the electronic structure calculations in the framework of the Korringa–Kohn–Rostoker coherent potential approximation overestimate the experimental peak splitting. This discrepancy is attributed to the shift of the intensity peaks with respect to the positions of the corresponding reciprocal-space minima of the effective interatomic interaction towards the (110) and equivalent positions. Combined with an assumption about monotonicity of the temperature behaviour of the splitting, such a shift implies an increase of the splitting with increasing temperature for all compositions considered in this study. The alpha-expansion calculations seem to confirm this conclusion.

1. Introduction

Almost a decade ago, Kulik *et al* [1] published their experimental results on electron diffraction from irradiated Cu–Pd alloys. In that study samples with 20, 22, 24 and 28 at.% Pd were maintained by high-energy electron irradiation in a steady disordered state away from their thermal equilibrium state at temperatures between 200 and 400 K. At these temperatures and compositions, equilibrium Cu–Pd alloys exhibit long-range order; the disordered state occurs only at much higher temperatures. In the equilibrium disordered state the intensity of diffuse scattering from Cu–Pd alloys with more than about 15 at.% Pd is characterized by the fourfold splitting of intensity peaks located at the (100), (110) and equivalent positions in the reciprocal space [1–7]. The resulting diffuse intensity distribution has maxima at the $(1q0)$ and equivalent positions (figure 1); the value of q increases with increasing Pd concentration. This fine structure of the diffuse scattering is caused by the atomic short-range order (SRO) and is a result of the indirect interaction of alloy atoms through conduction electrons in a situation in which an alloy has a reasonably well-defined Fermi surface with relatively flat areas [8, 9]. In this case the corresponding minima of

† Former name: I V Masanskii.

0953-8984/98/173791+16$19.50

the effective pair interatomic interaction in the reciprocal space are also split, and their separation is related to the wavevector $2\boldsymbol{k}_F$ which spans these flat areas of the Fermi surface.

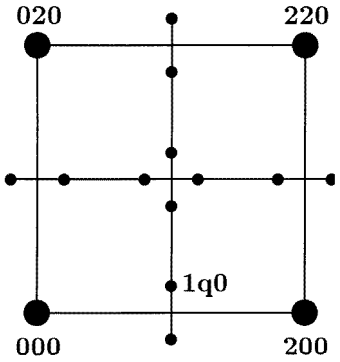

Figure 1. A schematic reciprocal-space picture of scattering from disordered Cu–Pd alloys. Large dots represent the Bragg reflections. Small dots correspond to the split diffuse intensity peaks.

Similar splitting of the diffuse intensity peaks was observed in the non-equilibrium steady disordered state under irradiation [1]. In addition to the expected concentration dependence of q, its variation with irradiation temperature was found. Even more curious was the qualitative change of the temperature dependence of the splitting with concentration: q decreased with increasing temperature in the case of 20, 22 and 24 at.% Pd, but this trend was reversed for the alloy with 28 at.% Pd for which an increase of the peak separation with temperature was found. At the same time, there was an increase of the scattering intensity with increasing temperature for all four compositions, contrary to the case of alloys at equilibrium where the intensity decreases with increasing temperature. A qualitative explanation of the temperature dependence of the splitting was proposed as follows. Firstly, the behaviour of the equilibrium SRO diffuse intensity in the case of the exactly solvable one-dimensional Ising model with competing antiferromagnetic nearest- and next-nearest-neighbour interactions was studied. It turned out that the peak positions varied with temperature. This result is in contrast with the mean-field-related Krivoglaz–Clapp–Moss (KCM) treatment [8, 10] which predicts temperature-independent peak positions at the minima of the interaction. As the intensity increased with decreasing temperature, the peak positions shifted towards the wavevector of the corresponding ground state. A similar result was obtained earlier for the two-dimensional ANNNI model using the cluster variation method [11]. It was concluded that the temperature dependence of the peak positions is a phenomenon which cannot be understood in the framework of mean-field theory. Secondly, the assumption was made that the behaviour of the diffuse intensity in irradiated Cu–Pd alloys was analogous to that of the equilibrium one-dimensional model. The only qualitative difference between the two cases was the opposite roles played by temperature. Based on this 'inverse-temperature hypothesis', the conclusion was drawn that one might expect to find the increase in q with temperature for the Cu–Pd alloy system at equilibrium. Here it may be added that the reversal of the temperature behaviour of the peak splitting could be expected according to this hypothesis as concentration increases, from the increase with temperature for 20, 22 and 24 at.% Pd to the decrease for 28 at.% Pd.

Last year, such an increase of the peak separation with temperature was observed

at equilibrium by Reichert *et al* [12] for the disordered Cu_3Au alloy. Moss and Reichert [13, 14] found the same behaviour by analysing the Monte Carlo simulation results of Roelofs *et al* [15] for the Cu–14.4 at.% Al alloy. In the latter work the inverse Monte Carlo pair interactions were determined from the experimental diffuse intensity at a single temperature and subsequently used to generate the Monte Carlo intensities at other temperatures. The theory of the temperature dependence of the splitting was proposed by Tsatskis [14, 16]; it identifies the wavevector dependence of the self-energy of the pair correlation function (PCF) as the origin of this effect. The self-energy $\Sigma(\boldsymbol{k})$ and the interaction term $2\beta V(\boldsymbol{k})$ enter the expression for the SRO diffuse intensity on an equal footing (equation (2.1*a*) below). In the KCM approximation the fact that the self-energy is a function of $\boldsymbol{k}$ is ignored. Apart from the observed increase in q with temperature, the possibility of the opposite behaviour, i.e., the decrease of the peak separation as temperature increases, was predicted. This is exactly what should be expected under equilibrium conditions for the Cu–28 at.% Pd alloy, if the inverse-temperature hypothesis is valid, although such temperature dependence was never seen experimentally. The possibility of the reversal of the temperature dependence of the peak splitting with increasing concentration seems to be indicated also by the results of the Monte Carlo simulations of Ozoliņš *et al* [17] for the first-principles alloy Hamiltonian with pair and multiatom interactions (25 at.% Pd) and the x-ray scattering measurements of Reichert *et al* [7] (29.8 at.% Pd). In both cases no (or a very small) change of the splitting with changing temperature was found.

The idea of the present study is to gain further insight into the behaviour of Cu–Pd alloys under irradiation by studying theoretically the evolution of the diffuse peak splitting with changing temperature in these alloys at equilibrium. More exactly, the aim is to find out whether the splitting increases with temperature in the range from 20 to 24 at.% Pd as the inverse-temperature hypothesis implies and whether this behaviour is reversed as concentration increases to 28 at.% Pd. Starting from the experimental SRO diffuse intensity measured at a particular temperature, we first solve the inverse scattering problem and calculate the effective interaction which is assumed to be pairwise and temperature independent. Then the direct problem is solved and the self-energy and diffuse intensity at different temperatures are calculated. The underlying theory of SRO is described in section 2. Section 3 considers data for Cu–Pd alloys existing in the literature. Finally, the results are discussed in section 4.

2. Alpha-expansion theory of SRO

We start by describing the theory of SRO which leads to the temperature-dependent peak splitting and is used in section 4 to relate the SRO diffuse intensities at different temperatures. This theory is based on the alpha expansion (AE) for the self-energy [16]; the self-energy is the only unknown quantity in the otherwise formally exact expression for the SRO intensity. The AE is the expansion in powers of SRO parameters α_{lmn}, hence the name. It was proposed as a generalizatiion of another approach to the calculation of the self-energy, the gamma-expansion method (GEM) [18–20], to deal with distant interactions which are essential in the case of the Fermi surface-related splitting. The complete set of the AE equations has the form

$$I_{SRO}(\boldsymbol{k}) = \frac{1}{c(1-c)\left[-\Sigma(\boldsymbol{k}) + 2\beta V(\boldsymbol{k})\right]} \tag{2.1a}$$

$$\Sigma(\boldsymbol{k}) = \Sigma_{000} + \sum_{lmn\neq 000} Z_{lmn}\Sigma_{lmn}\lambda_{lmn}(\boldsymbol{k}) \tag{2.1b}$$

$$\Sigma_{lmn} = a\alpha_{lmn}^2 + b\alpha_{lmn}^3 \qquad lmn \neq 000 \tag{2.1c}$$

$$\alpha_{000} = \frac{1}{\Omega}\int \mathrm{d}\boldsymbol{k}\ I_{SRO}(\boldsymbol{k}) = 1 \tag{2.1d}$$

$$\alpha_{lmn} = \frac{1}{\Omega}\int \mathrm{d}\boldsymbol{k}\ I_{SRO}(\boldsymbol{k})\lambda_{lmn}(\boldsymbol{k}). \tag{2.1e}$$

In equations (2.1) $\boldsymbol{k}$ is the wavevector, $I_{SRO}(\boldsymbol{k})$ is the SRO diffuse intensity in Laue units, c is the concentration, $\Sigma(\boldsymbol{k})$ is the self-energy of the PCF G (the latter is defined by equation (2.6) below), $\beta = 1/T$, T is the temperature in energy units, and $V(\boldsymbol{k})$ is the Fourier transform of the pair ordering potential

$$V_{ij} = \frac{1}{2}(V_{ij}^{AA} + V_{ij}^{BB}) - V_{ij}^{AB}. \tag{2.2}$$

The potential $V_{ij}^{\alpha\beta}$ corresponds to the interaction between an atom of type α at site i and an atom of type β at site j. Further, α_{lmn}, Σ_{lmn}, Z_{lmn} and

$$\lambda_{lmn}(\boldsymbol{k}) = Z_{lmn}^{-1}\sum_{\boldsymbol{r}\in lmn}\exp(\mathrm{i}\boldsymbol{k}\cdot\boldsymbol{r}) \tag{2.3}$$

are the SRO parameter, matrix element of the self-energy, coordination number and shell function for the coordination shell lmn, respectively, while α_{000} and Σ_{000} are the corresponding diagonal matrix elements. The summation in equation (2.1*b*) is performed over all coordination shells, whereas that in equation (2.3) is over the lattice vectors $\boldsymbol{r}$ belonging to the coordination shell lmn. The integration in equations (2.1*d*) and (2.1*e*) is carried out over the Brillouin zone of volume Ω. Coefficients a and b in equation (2.1*c*) are functions of concentration,

$$a = \frac{(1-2c)^2}{2[c(1-c)]^2} \tag{2.4a}$$

$$b = \frac{[1-6c(1-c)]^2 - 3(1-2c)^4}{6[c(1-c)]^3}. \tag{2.4b}$$

The SRO parameters α are proportional to the corresponding matrix elements of the PCF G,

$$G_{ij}^{AA} = G_{ij}^{BB} = -G_{ij}^{AB} = c(1-c)\alpha_{ij} \tag{2.5}$$

the definition of the PCF being

$$G_{ij}^{\alpha\beta} = \langle p_i^\alpha p_j^\beta\rangle - \langle p_i^\alpha\rangle\langle p_j^\beta\rangle \tag{2.6}$$

where p_i^α is the occupation number,

$$p_i^\alpha = \begin{cases} 1 & \text{atom of type } \alpha \text{ at lattice site } i \\ 0 & \text{otherwise} \end{cases} \tag{2.7}$$

and angular brackets denote statistical averaging.

The meaning of equations (2.1) is as follows. The first of equations (2.1*d*) and equation (2.1*e*) are the consequences of the fact that α_{ij} is the back Fourier transform of the intensity $I_{SRO}(\boldsymbol{k})$. Equation (2.1*b*) is the relation between the direct- and reciprocal-space representations of the self-energy. Equations (2.1*b*) and (2.1*e*) are written in coordination shell notations. The second of equations (2.1*d*) is the well-known sum rule [21] which reflects the property

$$p_i^\alpha p_i^\beta = p_i^\alpha \delta^{\alpha\beta} \tag{2.8}$$

of the occupation numbers following from their definition (2.7). The less obvious equation (2.1*a*) is one of the possible forms of the Dyson equation [22] which is satisfied by the PCF (2.6); this issue is discussed in considerable detail elsewhere [23]. The key equation is equation (2.1*c*) which closes the set of equations (2.1) by expressing the off-diagonal part of the self-energy in terms of the SRO parameters. Its right-hand side is, in fact, two first non-zero terms of a series expansion of Σ_{lmn} in powers of the SRO parameters. The latter are almost always sufficiently small, which justifies the expansion. These two terms were previously calculated [19, 20] in the framework of the GEM using self-consistent renormalization of the bare propagator $(\beta V)^{-1}$ in the generating functional for correlation functions [18]. The resulting expansion for the matrix elements of the self-energy was in powers of the matrix elements of the fully dressed propagator. This propagator is the PCF (2.6), and its matrix elements are therefore proportional to the corresponding SRO parameters. Thus, equations (2.1) form the set of self-consistent equations for the matrix elements of the self-energy (alternatively, Σ_{000} and α_{lmn}, $lmn \neq 000$, can be used as independent variables) and constitute the closed-form approximation for SRO. A particular AE approximation is defined by using equation (2.1*c*) for only a finite number of coordination shells and neglecting all other matrix elements of the self-energy. Another sequence of the AE approximations can be generated in the same way by taking into account only the lowest-order (quadratic) term in the AE expansion for Σ_{lmn} and ignoring the third-order contribution. For the rest of the paper both terms (as in equation (2.1*c*)) will be used. The AE is expected to be at least as accurate as the GEM, and the latter was used successfully in dealing with both direct and inverse diffuse-scattering problems [19, 20, 24], providing reliable results at almost all temperatures. The zero-order approximation of the AE is the well-known spherical model (SM) for correlations [25], also known under the name of the Onsager cavity field theory [26]. In the SM the self-energy is diagonal, i.e., wavevector independent; the single non-zero matrix element Σ_{000} is a function of temperature and concentration and is determined from the sum rule (2.1*d*).

In order to use equations (2.1) for calculating the evolution of the diffuse intensity with temperature and, in particular, the temperature dependence of the peak splitting, it is necessary to have information about the interaction V. It is assumed here that the interaction does not depend on temperature in the relevant temperature intervals; on the other hand, it is clearly concentration dependent, so a separate interaction set is needed for each alloy composition. We start from the set of the experimental SRO parameters and calculate the AE interaction in the reciprocal space by solving the inverse diffuse-scattering problem [19, 20]. This interaction can then be used for calculation of diffuse intensities at different temperatures and possibly, with much less confidence, at slightly different concentrations.

To solve the inverse problem, we rewrite equation (2.1*a*) as an expression for the interaction:

$$V_{AE}(\boldsymbol{k}) = \frac{T}{2}\left[\frac{I_{SRO}^{-1}(\boldsymbol{k})}{c(1-c)} + \Sigma(\boldsymbol{k})\right]. \tag{2.9}$$

The SRO diffuse intensity here is recalculated from the set of the experimental SRO parameters:

$$I_{SRO}(\boldsymbol{k}) = 1 + \sum_{lmn\neq 000} Z_{lmn}\alpha_{lmn}\lambda_{lmn}(\boldsymbol{k}). \tag{2.10}$$

In equation (2.10) the sum rule (2.1*d*) was used; otherwise, it is just the Fourier transformation written in coordination shell notation, similar to equation (2.1*b*). Substitution

of equations (2.1*b*) and (2.1*c*) into equation (2.9) shows that the only quantity in the resulting expression for $V_{AE}(\boldsymbol{k})$ which needs to be expressed in terms of the SRO parameters (or, equivalently, the SRO intensity) is the diagonal part Σ_{000} of the self-energy. The off-diagonal part of Σ is already an explicit function of the SRO parameters (equation (2.1*c*)). To find Σ_{000}, we integrate equation (2.9) over the Brillouin zone; this integration gives the diagonal direct-space matrix element of the integrand, as in equation (2.1*d*). The interaction V is an off-diagonal matrix in the direct space because of the absence of the self-interaction. Therefore, after the integration the left-hand side of equation (2.9) is zero and, as a result,

$$\Sigma_{000} = -\frac{\langle I_{SRO}^{-1}\rangle}{c(1-c)} \tag{2.11a}$$

$$\langle I_{SRO}^{-1}\rangle = \frac{1}{\Omega}\int \mathrm{d}\boldsymbol{k}\ I_{SRO}^{-1}(\boldsymbol{k}). \tag{2.11b}$$

Thus, equation (2.9) for the AE interaction can be written as

$$V_{AE}(\boldsymbol{k}) = V_{SM}(\boldsymbol{k}) + \frac{T}{2}\Sigma_{od}(\boldsymbol{k}) \tag{2.12}$$

where $\Sigma_{od}(\boldsymbol{k})$ is the Fourier transform of the off-diagonal part of the self-energy defined by equation (2.1*c*), and

$$V_{SM}(\boldsymbol{k}) = \frac{T}{2c(1-c)}\left[I_{SRO}^{-1}(\boldsymbol{k}) - \langle I_{SRO}^{-1}\rangle\right] \tag{2.13}$$

is the interaction obtained in the framework of the SM, i.e., in the zero-order AE approximation in which the off-diagonal part of the self-energy is zero. Note that, when compared with the interaction resulting from the KCM expression for $I_{SRO}(\boldsymbol{k})$ [8, 10],

$$V_{KCM}(\boldsymbol{k}) = \frac{T}{2c(1-c)}\left[I_{SRO}^{-1}(\boldsymbol{k}) - 1\right] \tag{2.14}$$

the SM interaction differs, at given c and T, only by the constant subtracted from the inverse intensity. Therefore, the off-diagonal direct-space interactions are identical in the KCM and SM approximations [20]. However, the KCM formula violates the sum rule (2.1*d*), thus leading to the appearance of the unphysical self-interaction

$$V_{000}^{KCM} = \frac{T}{2c(1-c)}\left[\langle I_{SRO}^{-1}\rangle - 1\right] \tag{2.15}$$

while in the SM, according to equation (2.13), this matrix element is zero. Returning to equation (2.12), every term in its right-hand side is expressed at this stage in terms of experimental data, and $V_{AE}(\boldsymbol{k})$ can be easily calculated.

3. Available data

We now consider previously published experimental and theoretical results for equilibrium Cu–Pd alloys in the range of concentrations discussed (20 to 30 at.% Pd). These results are of two types. Firstly, the electron and x-ray diffraction data and the results of the Korringa–Kohn–Rostoker coherent potential approximation (KKR-CPA) electronic structure calculations are available for the concentration dependence of the peak splitting. Secondly, for several alloy compositions large sets of the SRO parameters were determined by the Fourier inversion of the experimental SRO diffuse-scattering intensities. The latter type of data are used as input for the calculations of the kind described in section 2.

The peak separation q was measured at equilibrium for various concentrations and temperatures using electron [1–4] and x-ray [5–7] scattering. The splitting was observed

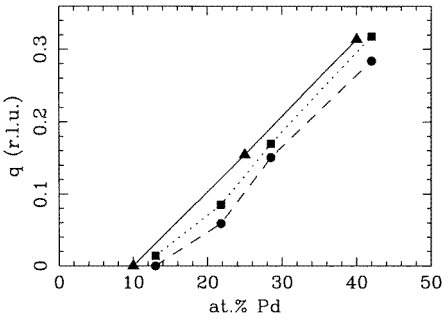

Figure 2. The concentration dependence of the peak splitting q as measured [5] in the x-ray diffraction experiment (circles, dashed line) and estimated [5] from the results of the KKR-CPA electronic structure calculations [27] (squares, dotted line). The data are taken from table 1 in [5]. The original KKR-CPA results [27] (triangles, solid line) are also shown. Straight lines connecting symbols are for eye guidance only. Note that all of the data were originally given in units of the distance between the (000) and (200) positions (equal to 2 r.l.u.) for the separation $m = \sqrt{2}q$ between the adjacent peaks.

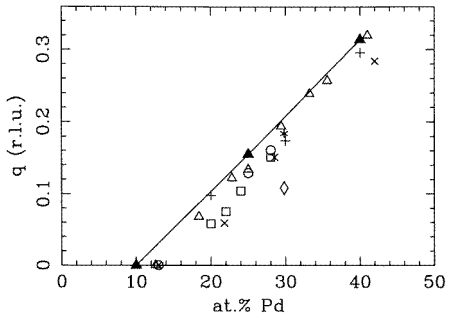

Figure 3. The same as figure 2, but all available experimental data are presented ([1]—open squares, about 800 K; [2]—open triangles, 773–893 K; [3]—open circles, about 700 K; [4]—plus signs, 1073 K; [5]—crosses, 1023 K; [6]—asterisk, 773 K; [7]—open diamond, about 700 K), in comparison with the KKR-CPA results [27] (filled triangles, solid line). The estimates made in [5] are not shown.

for alloys with more than about 15 at.% Pd, and it increased monotonically with increasing Pd content. Though very good agreement was noted by Gyorffy and Stocks (GS) [27] between the electron diffraction [2] and their KKR-CPA results, the calculated values of q were systematically slightly higher than the experimental ones. The discrepancy became noticeably larger in more recent measurements. In particular, Saha *et al* [5] compared their x-ray results for several compositions with the estimates that they made on the basis of the GS KKR-CPA calculations [27]. They found that the experimental splitting was smaller in all cases. The difference in q ranged from 0.014 to 0.034 reciprocal-lattice units (r.l.u.); 1 r.l.u. is the distance between the (000) and (100) positions. Their findings (table 1 in [5]) are shown in figure 2, together with the original GS results for different concentrations which were read off figure 2 in [27]. Surprisingly, all of the estimated values, presumably calculated by interpolating the results of [27], lie below the GS line; the reason for this is not clear. As a result, the disagreement between the experimental and theoretical values of q is even more pronounced than was reported in [5]. Figure 3 compares the KKR-CPA results

with the collection of all of the experimental data for the splitting known to the authors. It is seen that all the experimental points are located below the GS line. We propose an explanation for this discrepancy which is given in section 4.

Table 1. Data for three Cu–Pd alloys for which sets of the SRO parameters are available: T is the annealing temperature, N_α the number of the SRO parameters in the set, α_{000}^{exp} and q^{exp} the experimental values of α_{000} and q, respectively, and q^{rec} corresponds to the recalculated intensity (see the text). The splitting q is measured in r.l.u.

No	at.% Pd	Reference	T (K)	N_α	α_{000}^{exp}	q^{exp}	q^{rec}
1	21.8	[5]	1023	78	1.018	0.059	0
2	28.5	[5]	1023	78	1.014	0.151	0
3	29.8	[6]	773	72	1.786	0.184	0.162

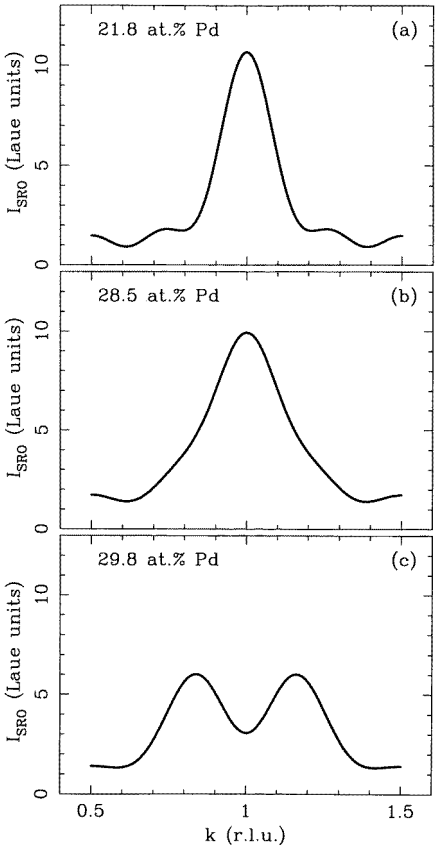

Figure 4. Profiles of the recalculated SRO diffuse intensities for the alloys 1 (a), 2 (b) and 3 (c) along the (h10) line. Variable k is a component of the wavevector $\boldsymbol{k} = (k, 1, 0)$. Note that there is no splitting of the (110) peak for the first two alloys.

Sets of the SRO parameters were obtained in the concentration interval considered for 21.8, 28.5 [5] and 29.8 [6] at.% Pd in x-ray experiments. The samples were annealed at some temperature corresponding to the disordered phase and then quenched. Hereafter these

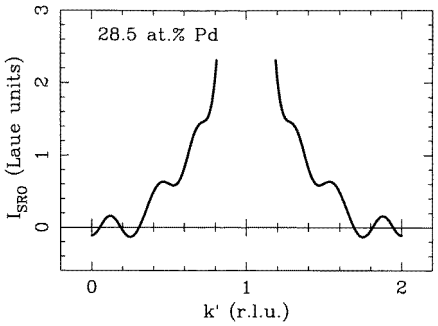

Figure 5. The recalculated SRO intensity along the (h00) line for the alloy 2 showing ranges of negative values. Variable k' is a component of the wavevector $\boldsymbol{k} = (k', 0, 0)$.

alloys will be referred to according to their numbers in table 1 which contains data used in the subsequent discussion. The splitting of the experimental (110) intensity peak was detected for all three compositions. The SRO parameters for large numbers of coordination shells were calculated by Fourier transforming the SRO part of the measured diffuse intensity after having separated it from other intensity contributions. We recalculated the SRO diffuse intensities for these three alloys using tables of the SRO parameters given in [5] and [6] and the theoretical value $\alpha_{000} = 1$ instead of the experimental values. Such substitution leads to a simple shift of the intensity and does not change its shape. Surprisingly, no splitting of the (110) peak was found in the recalculated SRO intensities for the alloys 1 and 2 (figures 4(a) and 4(b)); in the case of the alloy 2 this circumstance has already been noted elsewhere [28]. In addition, negative values of the recalculated SRO intensity were found for the alloy 2 (figure 5). The origin of all of these inconsistencies is probably the insufficient accuracy and/or number of the calculated SRO parameters. In contrast to these two cases, the recalculated SRO intensity for the alloy 3 shows the experimentally observed splitting (figure 4(c)). However, the corresponding value of q is noticeably smaller than the experimental result (table 1). As for the first two alloys, we find that the splitting tends to decrease after the recalculation. The accuracy of the recalculated intensity seems to be better for the alloy 3 as far as the magnitude of the splitting is concerned, though the deviation of the integrated intensity α_{000} from unity, which often serves as an accuracy criterion in diffuse-scattering experiments, is much larger than in two other cases (table 1).

4. Results and discussion

We assume that the discrepancy between the experimental and theoretical values of q discussed in section 3 is the result of the shift of the intensity peak position with respect to the position of the corresponding minimum of the interatomic interaction [16]. In other words, quantities which were measured and calculated were not the same. Indeed, what GS actually calculated [27] using the KKR-CPA method were the Fermi surfaces and, in particular, the Fermi wavevectors $\boldsymbol{k}_F$ along the (110) direction for different concentrations. These Fermi wavevectors were subsequently used to calculate the $2\boldsymbol{k}_F$-related separation $m = \sqrt{2}q$ between the adjacent minima of the interaction $V(\boldsymbol{k})$. Since the mean-field (KCM) description of correlations was chosen, the resulting separation between the intensity peaks was the same. However, it is generally different from the separation between the $V(\boldsymbol{k})$ minima and depends on temperature because of the temperature-dependent shift of

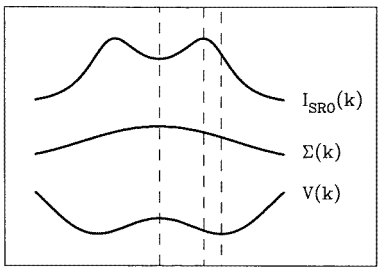

Figure 6. The shift of the intensity peak position as a result of the wavevector dependence of the self-energy. The behaviour of the SRO intensity, self-energy and interatomic interaction along the (h10) line is shown schematically. The self-energy profile is as found for the three Cu–Pd alloys discussed in the text (see figure 8 below). Dashed lines indicate the following positions (left to right): (110), the intensity peak, the minimum of the interaction.

the intensity peak position [16]. The shift itself is the consequence of the wavevector dependence of the self-energy (figure 6). This can be easily seen from either equation (2.1a) (the direct problem) or equations (2.12), (2.13) (the inverse problem). Consider, e.g., equation (2.1a); the $I_{SRO}(\boldsymbol{k})$ peak positions are determined by the condition $\boldsymbol{\nabla} I_{SRO} = 0$, which leads to

$$2\,\boldsymbol{\nabla} V = T\,\boldsymbol{\nabla}\Sigma \tag{4.1}$$

while the positions of the $V(\boldsymbol{k})$ minima are obtained from the equation $\boldsymbol{\nabla} V = 0$. It is clear from equation (4.1) that the extrema of $I_{SRO}(\boldsymbol{k})$ away from the special points are, in general, different from those of $V(\boldsymbol{k})$. On the other hand, if the approximate self-energy is $\boldsymbol{k}$-independent (as in the KCM or the SM approximations), then the two equations coincide and the intensity peak is not shifted. Figure 3 shows that the KKR-CPA calculations overestimate the experimental peak splitting everywhere in the range of concentrations from 20 to 30 at.% Pd. In the framework of the suggestion about the shift of the $I_{SRO}(\boldsymbol{k})$ peak being the origin of the disagreement between experiment and theory, this means that the intensity peaks are shifted towards the (110) position.

On the basis of this assumption, it is now possible to predict the temperature behaviour of the splitting if another, sufficiently reasonable assumption is made. We assume that the temperature dependence of the splitting is always monotonic (a non-monotonic behaviour was never observed experimentally). If this assumption is correct, then the direction of the shift at a particular temperature value can be related to its temperature dependence. At high temperatures, corrections to the KCM approximation are small, and the absolute value of the shift tends to zero, decreasing at least as T^{-1} with increasing temperature [16]. Therefore, in the case of the monotonic behaviour of the splitting the direction of the shift is the same at any temperature; the splitting increases with temperature, if the shift is towards the (110) position, and decreases otherwise. For Cu–Pd alloys this would mean that the splitting increases with temperature for all compositions in the range considered. This conclusion is in agreement with the one made on the basis of the inverse-temperature hypothesis [1] discussed in section 1 for alloys with 20, 22 and 24 at.% Pd, but it does not allow the change of the temperature behaviour predicted by this hypothesis for the Cu–28 at.% Pd alloy.

The next step is to check this prediction using the experimental data discussed in section 3. These data are quite limited, since sets of the SRO parameters are available only for three compositions. They are also not of sufficient accuracy for the reproduction of the fine structure of the (110) intensity peak. Only in one case, that of the alloy 3, is the

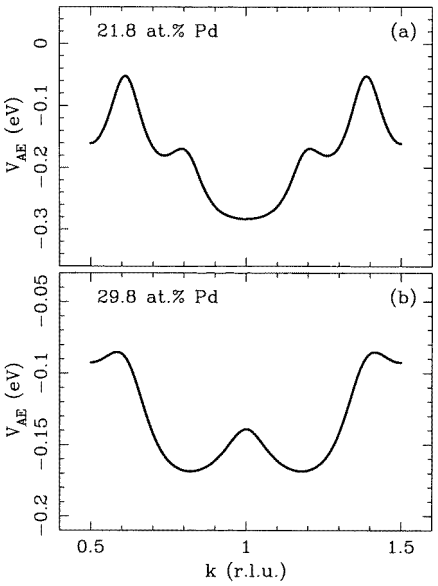

Figure 7. AE effective pair interactions $V_{AE}(\boldsymbol{k})$ along the $(h10)$ line for the alloys 1 (a) and 3 (b).

corresponding set good enough (i.e., contains a sufficient number of the reasonably accurate SRO parameters) to reproduce the experimentally observed splitting in the recalculated diffuse intensity (figure 4). Even in this case, the recalculation changes noticeably the magnitude of the splitting (see table 1). It seems that in this particular situation of the split intensity peaks, even larger sets of the more accurately determined SRO parameters are necessary. Nevertheless, the available sets can still be used to obtain information about the temperature dependence of the peak separation. The straightforward approach to this task described in section 2 is applicable only to the alloy 3. The solution of the inverse diffuse-scattering problem given by equations (2.12) and (2.13) cannot be obtained for the alloy 2, because the recalculated diffuse intensity becomes negative (figure 5); in this case the inverse intensity $I^{-1}_{SRO}(\boldsymbol{k})$ and, therefore, the effective interatomic interaction $V_{AE}(\boldsymbol{k})$ would contain unphysical singularities at those positions in the $\boldsymbol{k}$-space where the diffuse intensity vanishes. The inverse problem can be solved for the alloy 1, for which the recalculated intensity is always positive. However, in this case the resulting interaction which follows the shape of the intensity does not have a split minimum at the (110) position. The profiles of $V_{AE}(\boldsymbol{k})$ for the alloys 1 and 3 are shown in figure 7.

The easiest quantity to calculate in the framework of the AE theory of SRO is the direction of the shift. This can be done for all three alloys, despite problems with the data for two of them as indicated before. According to equation (4.1), the direction of the shift is determined by the reciprocal-space behaviour of the self-energy, and the latter can be easily obtained by Fourier transforming equation (2.1*c*), i.e., calculating $\Sigma_{od}(\boldsymbol{k})$, and using the experimental values of the SRO parameters. It is expected that the off-diagonal part of the self-energy is much less sensitive to the accuracy of the $\{\alpha_{lmn}\}$ set than the profile of the split intensity peak itself; there is no special reason for the self-energy to have any extrema away from the special points. Also, Σ_{od} is of second order in α_{lmn} (equation (2.1*c*)) and therefore decreases in the direct space faster than the PCF, which

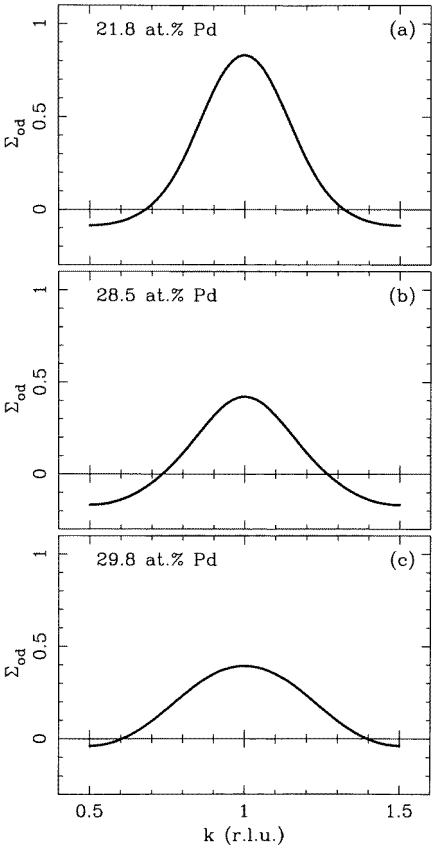

Figure 8. Profiles of the off-diagonal part $\Sigma_{od}(\boldsymbol{k})$ of the AE self-energy along the $(h10)$ line for the alloys 1 (a), 2 (b), and 3 (c). The maximal possible number N_α of coordination shells (table 1) was used in each case.

means that the distant SRO parameters are less important for its calculation. The results of such a calculation are presented in figure 8. The convergence of the results with respect to the number of coordination shells included in the AE approximation improves rapidly with increasing concentration; to achieve very good convergence, about 40, 20 and 5 shells are necessary for the alloys 1, 2 and 3, respectively. In all three cases $\Sigma_{od}(\boldsymbol{k})$ has a maximum at the (110) position, and from equation (4.1) it follows that the intensity peaks are shifted towards this position (see figure 6). This result is in agreement with our interpretation of the discrepancy between the experimental and the KKR-CPA values of q.

The actual value of the shift can be calculated only for the alloy 3, since for the other two alloys positions of peaks of the recalculated intensity and minima of the AE interaction are unavailable. The ten-shell AE approximation was used for this and all other calculations discussed in the rest of the paper. The result is 0.018 r.l.u.; it should be compared with the deviations of the experimental points from the GS line in figure 3. The deviation for the alloy 3 calculated by the linear interpolation of the GS results is 0.022 r.l.u., which is very close to the result obtained in the AE calculation. If we assume that the AE shift is about the same for both the experimental and recalculated intensities, then the position of the $V_{AE}(\boldsymbol{k})$ minimum for the former just falls on the GS line. The deviations of other

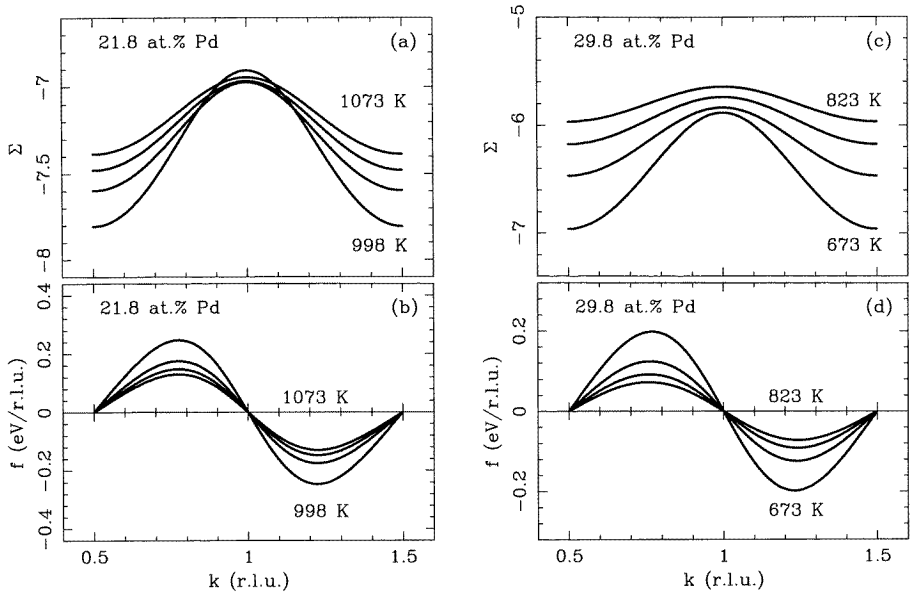

Figure 9. The AE self-energy $\Sigma(k)$ ((a), (c)) and the related function $f(k)$ defined by equation (4.2) ((b), (d)) along the $(h10)$ line for the alloys 1 ((a), (b)) and 3 ((c), (d)) at several equidistant temperatures. Indicated are maximal and minimal temperatures; the temperature steps are 25 K ((a), (b)) and 50 K ((c), (d)). The KCM values for the self-energy (equation (4.3)) are $\Sigma^{KCM} = -5.87$ (a) and $\Sigma^{KCM} = -4.78$ (c).

experimental points are of the same order of magnitude.

The change of the splitting with temperature can be analysed for the two cases (alloys 1 and 3) in which the inverse problem can be solved. This is done by calculating the self-energy as a function of temperature. Let us consider the profile of the self-energy along the $(h10)$ line. Along this line the self-energy is a function of just one component k of the wavevector $\boldsymbol{k} = (k, 1, 0)$. We define a function

$$f(k) = T\frac{\partial \Sigma}{\partial k} \tag{4.2}$$

whose temperature dependence, according to equation (4.1), determines that of the splitting. The functions $\Sigma(k)$ and $f(k)$ at different temperatures for the two alloys are displayed in figure 9. Accuracy checks show that the ten-shell approximation works very well for the alloy 3 and is still satisfactory (though noticeably worse) in the case of the alloy 1. Note that the AE results for the self-energy differ considerably from its KCM values; the KCM expression for the self-energy can be obtained, e.g., from the comparison of equations (2.9) and (2.14):

$$\Sigma^{KCM} = -\frac{1}{c(1-c)}. \tag{4.3}$$

In both cases the absolute value of $f(k)$ decreases with increasing temperature for any given value of k, which corresponds to the increase of the splitting with temperature. This result agrees with the conclusion based on the assumption of a monotonic temperature dependence of the splitting which was made earlier in this section.

Finally, a quantitative calculation of the temperature dependence of the intensity peak position q can be carried out, as before, for only one composition (alloy 3). The

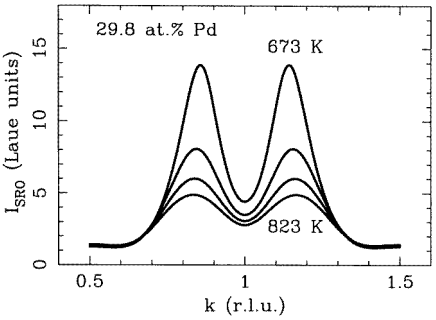

Figure 10. AE intensity profiles along the (h10) line for the alloy 3 at several equidistant temperatures. The temperature range and step are as in figures 9(c) and 9(d).

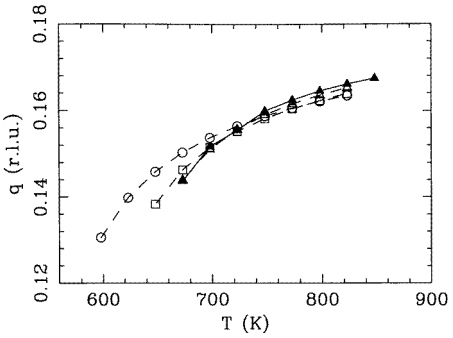

Figure 11. The intensity peak position q as function of temperature for the alloy 3 (filled triangles, solid line). The results for three other compositions (open symbols, dashed lines), 20 (circles), 24 (squares) and 28 (triangles) at.% Pd, calculated using the same AE interaction are also shown.

corresponding intensity profiles are presented in figure 10, while figure 11 shows results for the function $q(T)$ for this composition, as well as for three other concentrations covering the interval which was considered in [1]. In all of the calculations the same AE interaction (namely, that obtained by solving the inverse problem for the alloy 3; see figure 7(b)) was used. The aim was to find out whether the variation of composition for a concentration-independent interaction would lead to any particular change of the function $q(T)$. No such change takes place, as is seen from figure 11; the splitting increases monotonically with temperature for all four alloy concentrations.

In summary, we studied theoretically the temperature dependence of the Fermi surface-induced splitting of the (110) SRO diffuse intensity peak for Cu–Pd alloys under equilibrium conditions. The comparison was made with experimental observations for these alloys in a steady state under irradiation. The validity of the inverse-temperature hypothesis proposed previously to relate the two regimes was examined. At equilibrium this hypothesis predicts the qualitative change of temperature behaviour near the Cu_3Pd composition, namely, the increase of the splitting with increasing temperature in the composition interval 20 to 24 at.% Pd and its decrease with temperature as the concentration of Pd increases to 28 at.%. Comparing available electron and x-ray scattering data with the results of the KKR-CPA electronic structure calculations, we found that the theoretical approach overestimated the

experimental splitting. This disagreement was interpreted as the result of the shift of the diffuse intensity peaks with respect to the positions of the corresponding minima of the effective pair interatomic interaction towards the (110) position. An additional assumption about monotonicity of the temperature dependence of the splitting led to a connection between the direction and temperature behaviour of the peak shift. Under this assumption the shift towards the (110) position is equivalent to the increase of the splitting with increasing temperature. For Cu–Pd alloys this means that the splitting increases with temperature for all concentrations in the compositional range considered. This conclusion seems to be confirmed by the AE calculations, which are, however, based on limited experimental data. It agrees with the prediction of the inverse-temperature hypothesis for lower Pd concentrations (20 to 24 at.%) but, contrary to this prediction, does not allow any reversal of the temperature behaviour with increasing concentration of Pd. It also contradicts the results of recent computer simulations [17] and x-ray measurements [7] for higher Pd content (25 and 29.8 at.%, respectively), according to which the splitting is (almost) temperature independent. These results are consistent, on the other hand, with the reversal scenario. Among possible reasons for this disagreement are (i) limited validity of the inverse-temperature hypothesis, (ii) insufficient accuracy and/or size of the available sets of the experimental SRO parameters, (iii) the pair character of the interatomic interactions used in the AE theory of SRO and (iv) the approximate character of the AE calculations. Further direct measurements of the splitting as a function of temperature (as in [7]) for the range of compositions discussed are necessary to clarify the situation.

Acknowledgment

The authors would like to thank H Reichert and collaborators for communicating their experimental results [7] prior to publication.

References

[1] Kulik J, Gratias D and de Fontaine D 1989 *Phys. Rev.* B **40** 8607
[2] Ohshima K and Watanabe D 1973 *Acta Crystallogr.* A **29** 520
[3] Watanabe D 1959 *J. Phys. Soc. Japan* **14** 436
[4] Rodewald M, Rodewald K, De Meulenaere P and Van Tendeloo G 1997 *Phys. Rev.* B **55** 14 173
[5] Saha D K, Koga K and Ohshima K 1992 *J. Phys.: Condens. Matter* **4** 10 093
[6] Ohshima K, Watanabe D and Harada J 1976 *Acta Crystallogr.* A **32** 883
[7] Reichert H, Hung H H, Jahns V, Liang K S, Zehner D and Dosch H 1998 to be published
[8] Krivoglaz M A 1969 *Theory of X-Ray and Thermal Neutron Scattering by Real Crystals* (New York: Plenum)
Krivoglaz M A 1996 *Diffuse Scattering of X-Rays and Neutrons by Fluctuations* (Berlin: Springer)
[9] Moss S C 1969 *Phys. Rev. Lett.* **22** 1108
Moss S C and Walker R H 1974 *J. Appl. Crystallogr.* **8** 96
[10] Clapp P C and Moss S C 1966 *Phys. Rev.* **142** 418
Clapp P C and Moss S C 1968 *Phys. Rev.* **171** 754
[11] Finel A and de Fontaine D 1986 *J. Stat. Phys.* **43** 645
[12] Reichert H, Moss S C and Liang K S 1996 *Phys. Rev. Lett.* **77** 4382
[13] Moss S C and Reichert H 1996 private communication
[14] Reichert H, Tsatskis I and Moss S C 1997 *Proc. Joint NSF/CNRS Workshop on Alloy Theory (Strasbourg, 1996); Comput. Mater. Sci.* **8** 46
[15] Roelofs H, Schönfeld B, Kostorz G, Bührer W, Robertson J L, Zschack P and Ice G E 1996 *Scr. Mater.* **34** 1393
[16] Tsatskis I 1998 *J. Phys.: Condens. Matter* **10** L145
[17] Ozoliņš V, Wolverton C and Zunger A 1997 *Phys. Rev. Lett.* **79** 955
[18] Tokar V I 1985 *Phys. Lett.* **110A** 453

[19] Tokar V I, Masanskii I V and Grishchenko T A 1990 *J. Phys.: Condens. Matter* **2** 10 199
[20] Masanskii I V, Tokar V I and Grishchenko T A 1991 *Phys. Rev.* B **44** 4647
[21] See, e.g.,
Ducastelle F 1991 *Order and Phase Stability in Alloys* (Amsterdam: North-Holland)
[22] See, e.g.,
Izyumov Yu A and Skryabin Yu N 1988 *Statistical Mechanics of Magnetically Ordered Systems* (New York: Consultants Bureau)
[23] Tsatskis I 1998 *Local Structure from Diffraction (Fundamental Materials Science Series)* ed M F Thorpe and S J L Billinge (New York: Plenum)
[24] Reinhard L and Moss S C 1993 *Ultramicroscopy* **52** 223
Borici-Kuqo M and Monnier R 1997 *Proc. Joint NSF/CNRS Workshop on Alloy Theory (Strasbourg, 1996); Comput. Mater. Sci.* **8** 16
Le Bolloc'h D, Cren T, Caudron R and Finel A 1997 *Proc. Joint NSF/CNRS Workshop on Alloy Theory (Strasbourg, 1996); Comput. Mater. Sci.* **8** 24
[25] Joyce G S 1972 *Phase Transitions and Critical Phenomena* vol 2, ed C Domb and M S Green (New York: Academic)
Brout R 1965 *Phase Transitions* (New York: Benjamin)
[26] Onsager L 1936 *J. Am. Chem. Soc.* **58** 1468
Staunton J B and Gyorffy B L 1992 *Phys. Rev. Lett.* **69** 371
[27] Gyorffy B L and Stocks G M 1983 *Phys. Rev. Lett.* **50** 374
[28] Lu Z W, Laks D B, Wei S-H and Zunger A 1994 *Phys. Rev.* B **50** 6642